Ichthyology & Herpetology 114, No. 2, 2026, 283–298

A New Species of *Characidium* (Characiformes: Crenuchidae) from the Northwestern La Plata Basin in Argentina

Guillermo E. Terán[1,¶], V. Ezequiel Méttola[1,¶], Felipe Alonso[2], Martín M. Montes[3], Alejandro Méndez-López[1], Guido Miranda[4], Gastón Aguilera[1], and J. Marcos Mirande[1]

Using an integrative approach that combines molecular and morphological analyses, we describe *Characidium lilloi*, a new species from the Andean portion of the northwestern La Plata basin, specifically from the upper Bermejo and Juramento River basins in Argentina. Specimens were examined for morphometric, meristic, and osteological traits. Genetic analyses based on *COI* and *CYTB* sequences were conducted to infer its phylogenetic relationships. The new species is distinguished by a unique combination of morphological characters including an unscaled isthmus, absence of dark stripes or spots on fins, 7–13 regular transversal bars, 14 scales around the caudal peduncle, 35–37 scales in longitudinal series, and highly developed nasal flaps; and molecular evidence. *Characidium lilloi*, new species, was found to be closely related to *C. fasciatum* and *C. gomesi* and represents the first known member of the C2 Clade in the northwestern La Plata basin. Ecologically, *C. lilloi*, new species, inhabits fast-flowing mountain rivers within the Yungas and Chacoan. This discovery underscores the northwestern La Plata basin as a biogeographic hotspot of endemism and reinforces its importance as a high-priority area for freshwater conservation.

Utilizando un enfoque integrador que combina análisis moleculares y morfológicos, se describe *Characidium lilloi*, una nueva especie proveniente del sector andino del noroeste de la cuenca del Plata, específicamente de las cuencas altas de los ríos Bermejo y Juramento en Argentina. Los ejemplares fueron examinados en cuanto a caracteres morfométricos, merísticos y osteológicos. Se realizaron análisis genéticos basados en las secuencias de los genes mitocondriales *COI* y *CYTB* con el fin de inferir sus relaciones filogenéticas. La nueva especie se distingue por una combinación única de caracteres morfológicos incluyendo el istmo sin escamas, ausencia de bandas oscuras o manchas en las aletas, presencia de 7 a 13 barras transversales regulares, 14 escamas alrededor del pedúnculo caudal, 35 a 37 escamas en la serie longitudinal, y lóbulos nasales altamente desarrollados; y evidencia molecular. *Characidium lilloi*, nueva especie, se encuentra estrechamente relacionada con *C. fasciatum* y *C. gomesi*, y representa el primer miembro conocido del Clado C2 en el noroeste de la cuenca del Plata. Desde el punto de vista ecológico, *C. lilloi*, nueva especie, habita ríos de montaña de corriente rápida, dentro de las ecorregiones de las Yungas y el Chaco. Este hallazgo resalta al noroeste de la cuenca del Plata como un hotspot biogeográfico de endemismos, y refuerza su importancia como una región de alta prioridad para la conservación de ambientes dulceacuícolas.

THE genus *Characidium* (Crenuchidae) is one of the most species-rich and geographically widespread lineages of small characiforms in South America. It currently comprises over 80 valid species, with nearly half of them described in the last two decades (Stabile et al., 2024, 2025), reflecting ongoing efforts to document its hidden diversity. These fishes are broadly distributed across cis-Andean basins including the Amazon, Orinoco, São Francisco, and La Plata as well as trans-Andean systems such as the Maracaibo basin and the Pacific slopes of Colombia and Panama (Buckup, 1993a; Zanata et al., 2024). Some species of *Characidium* have been reported hovering over submerged vegetation in slow-flowing waters (Flausino et al., 2020), whereas others exhibit strong rheophilic tendencies, such as *C. crandellii* and *C. declivirostre*, which inhabit fast-running streams (Lujan et al., 2013; Lujan and Conway, 2015). This variation illustrates that the genus encompasses a broader ecological spectrum, ranging from short-bodied, slow-water species such as *C. rachovii* (see Travassos, 1952) to taxa specialized for rapid currents. They are morphologically characterized by elongate bodies and a dark blotch at the base of the middle caudal-fin rays—a trait that, while common, is homoplastically lost in several clades (Buckup, 1993b; Zanata et al., 2024). Phylogenetic analyses based on molecular markers have largely supported the monophyly of *Characidium sensu lato*, but they also reveal deep genetic structuring and unresolved relationships within the genus and among closely related genera such as *Microcharacidium*, *Leptocharacidium*, and *Melanocharacidium* (Oliveira-Silva et al., 2024; Serra et al., 2025).

The ichthyofauna of the northwestern portion of the La Plata basin, on the Atlantic slope of the central Andes,

[1] Unidad Ejecutora Lillo (UEL)–CONICET-Fundación Miguel Lillo, San Miguel de Tucumán, Argentina; ORCID: (GET) 0000-0002-3795-3345; (VEM) 0009-0009-3334-3927; (AML) 0000-0002-7251-7880; (GA) 0000-0002-5486-2787; and (JMM) 0000-0003-4370-3526; Email: (GA) gaguilera@lillo.org.ar. Send correspondence to GA.
[2] Instituto de Bio y Geociencias del NOA (IBIGEO-CONICET), Facultad de Ciencias Naturales, Universidad Nacional de Salta (UNSa), Salta, Salta Province, Argentina; ORCID: 0000-0001-7227-2732.
[3] Centro de Estudios Parasitológicos y de Vectores (CCT-CONICET–La Plata), Centro Científico Tecnológico, CONICET, La Plata–Consejo Nacional De Investigaciones Científicas y Técnicas, La Plata, Buenos Aires, Argentina; ORCID: 0000-0002-7177-333X.
[4] Wildlife Conservation Society, La Paz, Bolivia; ORCID: 0000-0002-8875-8005.
[¶] These authors made an equal contribution to this work and should be considered joint first authors.
Submitted: 5 August 2025. Accepted: 28 December 2025. Associate Editor: C. D. McMahan.
 DOI: 10.1643/i2025064 Published online: 23 June 2026

remains understudied but is increasingly recognized for its high levels of freshwater fish endemism (e.g., Terán et al., 2016; Alonso et al., 2024; Aguilera et al., 2025). This region includes the upper reaches of the Bermejo, Pilcomayo, and Juramento Rivers. These rivers mostly traverse the montane Yungas rainforest, where they display steep altitudinal gradients, clear rocky-bottomed channels, and marked seasonal floods associated with summer rainfall. Downstream, these systems transition into the lowland Chaco plains, where waters become increasingly turbid and sluggish, with sandy or muddy substrates and dense marginal vegetation. These pronounced environmental transitions, combined with the complex geological history of the region, act as effective ecological and dispersal barriers, contributing to population fragmentation, allopatric divergence, and local adaptation (Mirande et al., 2004, 2006; Terán et al., 2016, 2019; Alonso et al., 2024). Numerous recent studies have documented new species of fishes in this region, including several acestrorhamphids, loricariids, pseudopimelodids, callichthyids, and anablepids, restricted to headwater basins, some of which have been assessed as threatened under IUCN criteria (Calviño and Alonso, 2010; Mirande et al., 2011; Aguilera et al., 2019).

Several ichthyological surveys conducted in the upper Bermejo and Juramento basins, particularly in El Rey National Park and adjacent tributaries, have resulted in the discovery of specimens of *Characidium* that exhibited a distinctive combination of traits. Among them, most notably is the absence of scales on the isthmus—a condition not previously recorded in congeners from the northwestern La Plata River basin. Additional diagnostic characters in coloration, meristics, and osteology, along with molecular data (*COI* and *CYTB*), indicate that these specimens represent a distinct species of *Characidium*.

The objective of this study is to formally describe this new species of *Characidium* from the upper Bermejo and upper Juramento Rivers in northwestern Argentina. We apply an integrative taxonomic approach that combines external morphology, meristics, osteology, and mitochondrial DNA sequences to delimit the species and evaluate its phylogenetic relationships. Furthermore, we provide information on the species' habitat, explore its ecological and biogeographic context, and evaluate conservation status in light of the environmental challenges affecting freshwater ecosystems in the northwestern La Plata basin.

MATERIALS AND METHODS

Fish sampling.—Specimens were collected using hand nets and electrofishing to minimize environmental disturbance. Measurements were taken to reduce pain or discomfort during handling. Fish were euthanized by immersion in an anesthetic solution (0.1% 2-phenoxyethanol), then fixed in a 4% formaldehyde solution for one week. Following fixation, specimens were washed in water for 24 hours and transferred to 70% ethanol for long-term preservation.

For genetic analysis, small tissue samples were taken from freshly anesthetized specimens and immediately preserved in absolute ethanol. These tissue samples were deposited in the tissue collection of the Fundación Miguel Lillo (CIT-FML), which is associated with its ichthyological collection (CI-FML), for future reference. All procedures followed the ethical guidelines and animal welfare regulations established by the Comité Nacional de Ética en la Ciencia y Tecnología, Argentina. Acronyms follow Sabaj (2020) with the addition of CIT-FML, which is stated above.

The material examined in this study derives from specimens deposited in museum collections. Part of the material originates from National Parks, collected under the following permits: Rey National Park, Salta (DRNOA 149/2018 Mod.1, IF-2019-75047775; DRNOA 226/22, IF0-2023-123289558); other localities within the basin (Res. No. 000101, Expte. No. 227-176829/2022-0); and Calilegua National Park, surrounding areas, Jujuy (Res. No. 101/2023).

Morphological and osteological analyses.—Morphological data were derived from comparative material and the original descriptions of closely related species. Measurements were performed point-to-point using digital calipers with an accuracy of 0.1 mm. Morphometric and meristic counts followed Buckup (1993a), Melo and Oyakawa (2015), and Méttola et al. (2025).

For osteological analysis, five specimens were cleared and stained (CS) according to the protocol established by Taylor and Van Dyke (1985). The terminology used for osteological structures follows Weitzman (1962), with the exception of anterior and posterior ceratohyal instead of ceratohyal and epihyal, anguloarticular and retroarticular rather than articular and angular (Nelson, 1969, 1973), vomer replacing prevomer (Roberts, 1969), mesethmoid and endopterygoid for ethmoid and mesopterygoid, respectively (Fink and Fink, 1981, 1996). In the morphological description, the holotype counts are marked with an asterisk (*), and the number of specimens examined for each meristic character is provided in parentheses.

DNA extraction, amplification, and sequencing.—Total genomic DNA was extracted from muscle tissue samples of three specimens, which had been preserved in cold 96% ethanol. The extraction was performed using the PURO-Genomic DNA kit, manufactured by PB-L Productos Bio-Logicos S.A., following the manufacturer's protocol. The partial mitochondrial cytochrome oxidase subunit 1 (*COI*) gene was amplified using polymerase chain reaction (PCR) on an Eppendorf Mastercycler thermal cycler. The amplification utilized the primers Fish F1 (5′–TCA ACC AAC CAC AAA GAC ATT GGC AC–3′) and Fish R1 (5′–AGA CTT CTG GGT GGC CAA AGA ATC A–3′), as described by Ward et al. (2005). PCR procedures followed the protocols outlined by Souza-Shibatta et al. (2018). The fragment of *CYTB* was amplified with the forward primer CB3-H (5′–GGC AAA TAG GAA RTA TCA TTC–3′) and reverse primer Gludg-L (5′–TGA CTT GAA RAA CCA YCG TTG–3′; Palumbi et al., 1991) following thermocycling conditions as described by Loureiro et al. (2018). Sequencing of PCR products was performed bidirectionally (forward and reverse) using an ABI 3730XL sequencer (Macrogen Inc., Korea) to ensure sequence accuracy and completeness.

Molecular data analyses.—Sequences were aligned using MUSCLE (Edgar, 2004) in MEGA (Kumar et al., 2018), which was also used to calculate genetic distances for the *COI* marker under the Kimura 2-parameter (K2) substitution model, as it is the standard for DNA barcoding datasets (Díaz et al., 2016), for comparative purposes.

Phylogenetic reconstruction was conducted using TNT for parsimony analysis and IQ-TREE for maximum likelihood (ML) analysis. The dataset comprised sequences from Méttola et al. (2025), Serra et al. (2025), Stabile et al. (2024), Zanata et al. (2024), and Oliveira-Silva et al. (2024). Phylogenetic reconstruction was based on *COI* and the combination of *COI* + *CYTB*. Complete list of sequences in Supplemental Table S1 (see Data Accessibility).

Parsimony analysis was performed in TNT under extended implied weighting (Goloboff, 1993, 2014), exploring K values (3–27) that imply a broad range from strong to mild weighting against the homoplasy (Goloboff, 1993). For comparative purposes, we also analyzed the dataset under equal weighting. Clade support was assessed using symmetric resampling with 10,000 replicates, and results are expressed as GC values (groups present/contradicted; Goloboff et al., 2003). Calculations of support were done under extended implied weighting and K = 10, which is a relatively mild weighting against the homoplasy for this dataset. Under this K-value, an average homoplastic character has about 77% of the weight of a character with no homoplasy in the analyzed dataset.

Maximum likelihood (ML) analyses were conducted in IQ-TREE (Trifinopoulos et al., 2016). The best-fitting nucleotide substitution models were selected according to the Bayesian information criterion (BIC). For the *COI* dataset, the TIM2 + F + I + G4 model was identified as the best substitution model (Kalyaanamoorthy et al., 2017). For the concatenated *COI* + *CYTB* dataset, partitioned models were applied (Chernomor et al., 2016). Specifically, the best models for the *COI* codon positions were TN + I + G4 (first position), F81 + F (second position), and TN + F + G4 (third position). For *CYTB*, the best models were K3Pu + R2, HKY + F + I, and TN + F + G4 for the first, second, and third codon positions, respectively. Node support was assessed using ultrafast bootstrap with 10,000 replicates (Hoang et al., 2018).

Nomenclatural acts.—This electronic publication complies with the provisions of the International Code of Zoological Nomenclature (ICZN), ensuring that the new taxonomic names proposed herein are valid from the electronic version of the article. All nomenclatural acts presented have been duly registered with ZooBank, the ICZN's official registry. The Life Science Identifiers (LSIDs) assigned to these acts can be accessed by appending them to the URL prefix "https://zoobank.org/". The LSID for this work is: urn:lsid:zoobank.org:pub:5FB9AFF4-B64C-42F0-BDE0-46C3B6B57FF0.

Characidium lilloi, new species

urn:lsid:zoobank.org:act:8D480EFB-8AC7-4581-923F-7860A1F429DD

Figures 1–4, Table 1

Holotype.—CI-FML 8195, 51.8 mm SL, Argentina, Salta Province, Anta, Río Popayán at El Rey National Park, Del Valle River basin, 24°43′53.8″S, 64°34′21.6″W, G. Terán, G. Aguilera, F. Alonso, A. Méndez-López, and B. Bugeau, October 2022.

Paratypes.—All from Argentina. CI-FML 8196 (CIT-FML 00432), 6, 36.8–51.8 mm SL, IBIGEO 550, 6, 38.7–46.8 mm SL, both collected with the holotype; CI-FML 5366, 2, 54.9–67.1 mm SL, Salta Province, San Ramón de la Nueva Orán, Blanco River, Bermejo River basin, 23°07′13″S, 64°29′16″W, J. M. Mirande, G. Terán, and F. Alonso, July 2014; CI-FML 8197, 7, 32.5–52.4 mm SL, Jujuy Province, Ledesma, San Lorenzo River, tributary to San Francisco River, Bermejo River basin, 23°49′45.5″S, 64°39′05.5″W, G. Terán, G. Aguilera, and D. Delgado, December 2016; CI-FML 8198, 1, 43.1 mm SL, Jujuy Province, Ledesma, Lavallén River under bridge of vecinal road, San Francisco-Bermejo River basin, 24°02′43.7″S, 64°42′00.6″W, M. Casalinuovo, G. Terán, and G. Aguilera, August 2019; CI-FML 8199 (CIT-FML 00707), 1, 53.2 mm SL, Salta Province, Anta, Guanaco River, Juramento River basin, 25°04′22.3″S, 64°38′46.6″W, M. Casalinuovo, October 2019; CI-FML 8200, 2, 38.9–41.2 mm SL, Salta Province, Metán, Juramento River basin, 25°13′0″S, 64°28′0″W, F. Cancino and G. Aguilera, August 2013; CI-FML 8201, 6 (3 CS), 38.2–57.6 mm SL, Salta Province, Anta, Río Popayán at El Rey National Park, Del Valle River basin, 24°43′53.8″S, 64°34′21.6″W, G. Terán, G. Aguilera, F. Alonso, and B. Bugeau, October 2019; CI-FML 8202, 1, 43.8 mm SL, Salta Province, General San Martín, stream tributary to Itaú River, near Campo Largo, Río Bermejo basin, 22°01′34″S, 63°56′06″W, G. Terán, F. Alonso, and J. M. Mirande, January 2014; CI-FML 8203, 2 (CS), 24.6–24.8 mm SL, Salta Province, San Ramón de la Nueva Orán, Quebrada Colorada stream at RN50, Bermejo River basin, 22°48′12″S, 64°21′10″W, G. Terán, F. Alonso, and J. M. Mirande, May 2015; CI-FML 8204, 10, 47.8–57.6 mm SL, Jujuy Province, Ledesma, unnamed stream, tributary of Sauzalito stream at Calilegua National Park, San Francisco-Bermejo River basin, 23°38′28.4″S, 64°36′11.0″W, G. Terán, G. Aguilera, M. A. Cortés, and A. Méndez-López, November 2024; IBIGEO 551, 5, 40.3–63.3 mm SL, Río Dorado, Bermejo River basin, 24°38′50.2″S, 64°22′31.9″W, F. Alonso, G. Terán, and M. Waldbillig, May 2023; MACN-Ict 13514, 3, 42.7–50.2 mm SL, Salta Province, Güemes, Mojotoro River, Bermejo River basin, 24°43′53.8″S, 65°01′42.0″W, M. Casalinuovo, October 2023.

Non-type material.—All from Argentina. CI-FML 7771, 41 (2 stained), 20.4–26.3 mm SL, Jujuy Province, San Francisco River, 23°42′43″S, 64°32′09″W, M. Casalinuovo, August 2019; CI-FML 8194, 8 (4 stained, 1 CS), 44.8–65.1 mm SL, Jujuy Province, Ledesma, Ledesma River, 23°57′27.4″S, 64°55′41.4″W, M. Casalinuovo, May 2019; CI-FML 8205 (CIT-FML 045), 9, 20.30–25.33 mm SL, Jujuy Province, Ledesma, San Francisco River, Bermejo River basin, 23°42′43″S, 64°32′09″W, G. Terán, G. Aguilera, F. Alonso, and J. M. Mirande, September 2016.

Diagnosis.—*Characidium lilloi* is distinguished from all congeners except *C. alipioi*, *C. amaila*, *C. crandellii*, *C. cricarense*, *C. declivirostre*, *C. duplicatum*, *C. grajahuense*, *C. hasemani*, *C. helmeri*, *C. iaquira*, *C. japuhybense*, *C. kalunga*, *C. kamakan*, *C. krenak*, *C. lanei*, *C. lauroi*, *C. nambiquara*, *C. oiticicai*, *C. pterostictum*, *C. schubarti*, *C. summus*, *C. tatama*, *C. timbuiense*, *C. travassosi*, *C. vidali*, *C. wangyapoik*, and members of the *C. fasciatum* group or Clade C2 (Buckup, 1993b)—*C. boavistae*, *C. bolivianum*, *C. gomesi*, *C. fasciatum*, and *C. purpuratum*—by having the isthmus unscaled (Fig. 3). It can be distinguished from *C. crandellii*, *C. declivirostre*, *C. duplicatum*, *C. iaquira*, *C. summus*, and *C. wangyapoik* by isthmus and area between pectoral fins unscaled (vs. unscaled area from the isthmus to the pelvic girdle); from *C. alipioi*, *C. grajahuense*, *C. hasemani*, *C. kamakan*, *C. krenak*, *C. lanei*, *C. nambiquara*, *C. pterostictum*, *C. timbuiense*, and *C. vidali* by the absence of well-defined dark stripes or spots on caudal and anal fins (vs.

Fig. 1. *Characidium lilloi*. CI-FML 8195. Holotype, 51.8 mm SL. Lateral views of the live and preserved specimen; dorsal and ventral views shown only for the preserved specimen. Scale bar = 1 cm.

Fig. 2. Lateral views of live paratypes of *Characidium lilloi*. CI-FML 8196, 36.8–49.1 mm SL, Argentina, El Rey National Park, Río Popayán. Scale bar = 1 cm.

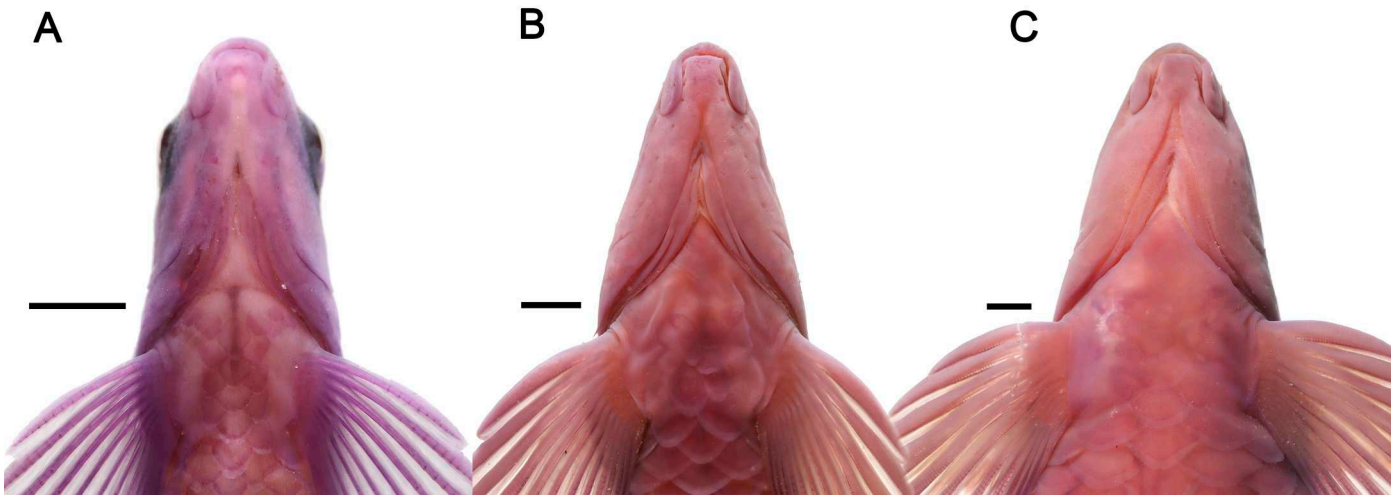

Fig. 3. Ontogenic variation of isthmus squamation in *Characidium lilloi*. (A) Smaller specimen (CI-FML 7771, 24.2 mm SL) lacking scales on isthmus but showing a row of scales between pectoral fins. Larger specimens with rudimentary scales between pectoral fins (CI-FML 8194, B: 44.8 mm SL; C: 65.1 mm SL). Scale bar = 1 mm.

presence of dark gray spots or stripes); from *C. helmeri*, *C. japuhybense*, *C. lauroi*, *C. oiticicai*, *C. travassosi*, and *C. schubarti* by the absence of dashes or spots on flanks (vs. presence of spots or dashes); from *C. amaila* and *C. kalunga* by the presence of vertical bars that are wider near the dorsum and extend ventrally to the lateral line (vs. irregular pattern or offset arrangement of dorsal and ventral halves); and from *C. tatama* by the presence of 14 scales around the peduncle (vs. 12 or fewer).

Characidium lilloi is distinguished from remaining members of the *C. fasciatum* group (C2 clade from Buckup, 1993b) by having 35 or more lateral-line scales (vs. 34 or less in *C. purpuratum* and *C. boavistae*); by the absence of well-defined dark stripes on the caudal fin (vs. presence of distinct stripes in *C. gomesi*); and by highly developed nasal flaps, posterior flap overlapping and almost touching the anterior flap (Fig. 4; vs. poorly developed nasal flaps in *C. bolivianum* and *C. fasciatum*). Additionally, *C. lilloi* further differs from *C. fasciatum* by the foramen in the pterosphenoid bone occupying about half of the space (vs. only one-fourth); from *C. fasciatum* and *C. gomesi* by lacking faint thin stripes between the longitudinal stripe and the pre-dorsal scales (vs. presence); from *C. bolivianum* by having 9–10 branched pectoral fin-rays (vs. 7–8 branched rays) and the maxilla not reaching the anterior orbit margin (vs. reaching or slightly surpassing it).

Fig. 4. Narines of *Characidium lilloi* (CI-FML 8197, 47.8 mm SL). Nares independent but close to each other, highly developed flaps. Scale bar = 1 mm.

Description.—Morphometric data summarized in Table 1. Body elongate, relatively compressed laterally. Lateral view slightly convex from snout tip to dorsal fin; relatively straight along dorsal-fin base; slightly decreasing from this point to caudal fin, with slight prominence at adipose fin. Ventral profile convex from snout tip to pelvic-fin insertion; straight from pelvic-fin insertion to anal-fin origin; rising prominently at anal-fin base, and relatively straight to caudal fin. Greatest body depth at or just before dorsal-fin origin.

Snout triangular in lateral view. Mouth subterminal. Distal tip of maxilla not reaching transversal plane through anterior margin of orbit. Orbit circular, larger than snout length, smaller than maxilla. Iris almost rounded, with anteroventral projection. Nares close to each other, flaps well developed and almost touching each other (Fig. 4).

Lateral line completely pored with 35(14)*, 36(13), or 37(8) scales. Scales above lateral line 4(26)* or 5(10); below lateral line 4(35)*. Predorsal scales 9(3), 10(17)*, 11(12), or 12(3). Circumpeduncular scales 14(35)*. Isthmus and area between pectoral fins unscaled. Ontogenetic variation observed in the squamation, with smaller specimens lacking scales on isthmus but showing a row of scales between pectoral fins, and larger specimens with rudimentary scales between pectoral fins (Fig. 3).

Dorsal-fin rays ii8(1), ii9(33)*, or ii10(1); anal-fin rays ii6(13), ii7(22)*; pectoral-fin rays iii9(17) or iii10(17)*; pelvic-fin rays i7(3) or i8(32)*; principal caudal-fin rays i9,8i(35)*.

Pseudotympanum and swimbladder.—*Pseudotympanum* present, relatively small, bounded dorsally by *lateralis superficialis*, anteriorly and posteriorly by *obliquus inferioris*, and ventrally by *obliquus superioris* muscles. Humeral hiatus divided into anterior and posterior chambers by pleural rib

Table 1. Morphometric data of *Characidium lilloi*, new species. Mean and range include the holotype and 30 paratypes. SD = standard deviation.

Character (mm)	Abbreviation	Holotype	Mean	Range	SD
Total length	TL	63.8	55.1	31.0–74.5	8.4
Standard length	SL	51.8	45.6	25.2–63.3	7.4
Head length	HL	12.9	11.1	6.0–14.8	1.8
Percentage of standard length					
Head length	HL%	24.8	24.0	22.9–25.6	0.7
Head height	HH	14.0	13.3	11.7–15.8	0.8
Head width	HW	9.6	8.5	7.6–10.0	0.6
Pre-pectoral distance	PPD	22.1	21.9	20.0–25.8	1.3
Pectoral-fin height	PFH	17.5	18.9	15.9–22.0	1.4
Pectoral-fin length	PFL	26.9	26.0	23.1–28.7	1.5
Pre-dorsal distance	PDD	46.5	45.8	43.0–49.0	1.2
Dorsal-fin height	DFH	17.0	18.0	15.5–20.4	1.4
Dorsal fin length	DFL	29.0	27.6	14.8–31.8	3.9
Dorsal-fin base	DFB	16.9	16.3	14.1–18.3	1.0
Pre-pelvic distance	PPVD	51.7	51.9	48.9–55.9	1.5
Pelvic-fin height	PVFH	10.9	11.9	10.4–14.2	0.9
Pelvic-fin length	PVFL	22.5	21.8	18.8–24.0	1.3
Pre-anal distance	PAD	76.9	74.6	67.7–78.9	2.2
Anal–apex distance	AAD	96.8	94.6	89.9–99.2	2.0
Anus to anal fin distance	AAFD	6.4	6.6	4.7–7.9	0.6
Anal-fin height	AFH	16.0	16.4	14.1–19.8	1.3
Anal-fin length	AFL	20.9	20.0	17.2–22.1	1.2
Anal-fin base	AFB	7.8	7.3	5.8–8.2	0.6
Pre-adipose distance	PADD	83.0	82.0	79.5–84.7	1.5
Adipose-fin height	AFH	5.7	6.4	5.4–7.5	0.6
Peduncle length	PL	19.9	19.6	16.7–21.7	1.0
Peduncle width	PW	3.1	2.6	1.8–4.0	0.6
Body depth at dorsal-fin origin	BDDFO	24.0	22.6	18.0–26.0	2.0
Body depth at anal-fin origin	BDAFO	19.0	18.3	16.0–20.7	1.2
Body depth at caudal peduncle	BDCP	13.8	12.7	11.1–13.9	0.8
Body width	BW	12.2	10.9	7.9–12.5	1.0
Percentage of head length					
Snout length	SNL	21.5	23.1	20.2–25.4	1.4
Snout–maxillary tip	SMT	26.0	25.2	22.8–27.1	1.0
Anterior naris–orbit	ANO	6.5	7.0	5.9–8.2	0.6
Posterior naris–orbit	PNO	3.7	4.3	2.9–6.4	0.9
Cheek	CH	9.3	8.5	5.7–10.6	1.1
Orbital diameter	OD	21.5	23.8	19.6–33.6	2.7
Interorbital diameter	IOD	11.5	11.2	9.6–12.9	1.0

of fifth vertebra, in a 40/60 proportion, respectively. Second rib covered by muscle (Fig. 5).

Swimbladder with two chambers, anterior chamber bilobate and short, and posterior chamber smaller than anterior.

Osteology.—Mesethmoid long and narrow, its anterior portion only contacting premaxillae, separated from vomer and palatines by a block of cartilage; posterior region reaching frontals dorsally and lateral ethmoids ventrally. Frontals articulated to each other almost through their entire length, completely obliterating frontal fontanel, which is consequently absent. Parietal fontanel trapezoidal or triangular, limited only anteriorly by frontals, almost restricted to parietal area. Rhinosphenoid and orbitosphenoid separated from parasphenoid. Pterosphenoid with a large conspicuous rounded or ovated foramen; ventral portion receiving dorsal projections of parasphenoid. Pterotic longer anteroposteriorly, auditory foramen present.

Dentary not overlapping anguloarticular and separated from retroarticular. Quadrate dorsal arm considerably wider than horizontal arm; articular foramen present. Symplectic lamella developed posterodorsally, laterally covering tip of quadrate horizontal arm in larger specimens (44.0–54.7 mm SL). Metapterygoid ventral cartilage extensively contacting symplectic; posterior portion overlapping anterior concavity of hyomandibula. Mesopterygoid not reaching palatine, joined to ectopterygoid on its entire lateral border. Palatines long and rectangular, reaching or surpassing anterior border of vomer. Hyomandibula posterodorsally extended, its articular condyle almost at dorsal edge of opercle.

Maxilla toothless. Premaxilla with 6(5) conical to tricuspid teeth (Fig. 6A). Dentary teeth arranged in two rows: external row with 8(3), 10(1), or 11(1) teeth, gradually decreasing in size posteriorly, anterior three to four large teeth tricuspid; internal row with 15(2), 18(1), 19(1), or 20(1) conical teeth (Fig. 6B). Ectopterygoid with one row of 10(1), 11(2), or 13(2) minute and conical teeth. Endopterygoid teeth absent.

Supraorbital present, not contacting antorbital. First infraorbital laterosensory tube with dorsal and anterior branches,

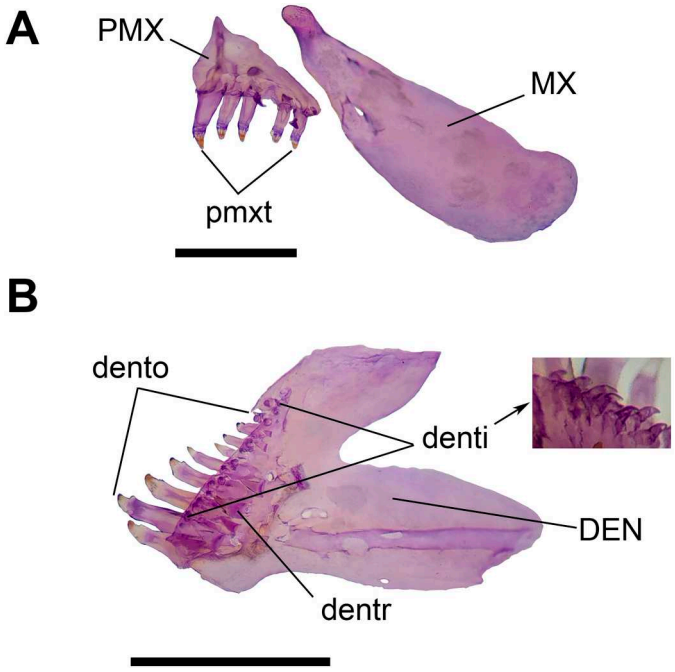

Fig. 5. (A) Right upper jaw in medial view of *Characidium lilloi* (CI-FML 8201, 54.9 mm SL). (B) Right dentary jaw in medial view. Abbreviations: DEN, dentary; denti, inner dentary teeth; dento, outer dentary teeth; dentr, replacement teeth; MX, maxillary; PMX, premaxillary; pmxt, premaxillary teeth. Scale bar = 1 mm.

an additional ventral branch present in larger specimens (44.0–54.7 mm SL); developed anterior and dorsoposterior lamellae, the latter contacting anterior portion of antorbital forming anterior margin of eye. Second infraorbital with developed ventral laminar portion below laterosensory canal. Remaining orbital series reduced to the ossified laterosensory tubes and pores io3 to io6, posteriorly connected with sphenotic canal.

Nasal bones restricted to an ossified canal. Epiphyseal branch of supraorbital canal present. Parietal branch of supraorbital canal also present, extending well beyond limit between frontal and parietal bones, but not reaching supratemporal canal. Dentary canal over its ventral portion, initiating below alveolar region of medialmost teeth to the posterior edge of the bone, where it continues through anguloarticular and preopercle. Preopercular canal exiting bone at hyomandibular condyle. Extrascapular receiving pterotic and supratemporal canals. Posttemporal posterior canal branch present. Supracleithrum with an additional exit dorsal to that for the lateral line.

Postcleithrum 1 absent, postcleithrum 2 laminar, located at the posterior tip of cleithrum. Postcleithrum 3 slender and long, passing posteroventral base of pectoral fin. First dorsal-fin pterygiophore inserted after neural process of vertebrae 10(4) or 11(1). Tip of pelvic bone just behind fifth pair of ribs. First anal-fin pterygiophore between haemal spines of vertebrae 22 and 23(5). Caudal fin with 7(2) or 8(3) dorsal and 6(2) or 7(3) ventral procurrent rays.

Branchiostegal rays 5(4) or 6(1); anterior three or four attached to the ventral edge of anterior ceratohyal, posteriormost two joined to the lateral surface of posterior ceratohyal and epihyal, respectively. Gill rakers on first gill arch 16; 9(5) on hypobranchial plus ceratobranchial, 6(5) on epibranchial plus first pharyngobranchial, and one at the angle between them.

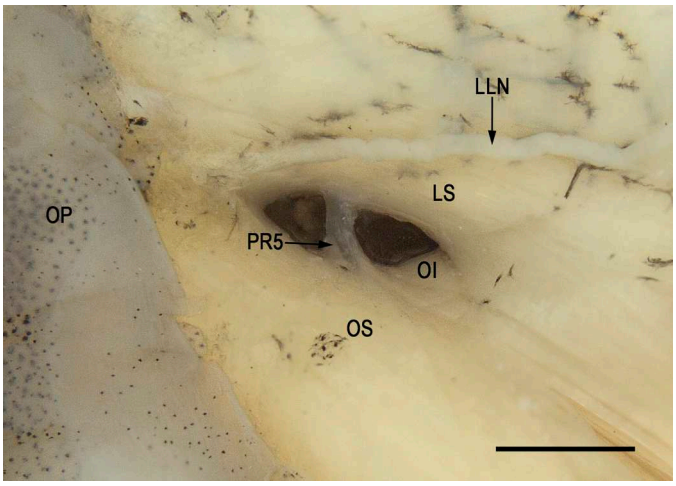

Fig. 6. Pseudotympanum of *Characidium lilloi* (CI-FML 8196, 50.8 mm SL) in left lateral view. Humeral hiatus divided into anterior and posterior chambers by pleural rib of fifth vertebra. LLN: lateral line nerve; LS: *lateralis superficialis*; OI: *obliquus inferioris*; OP: opercle; OS: *obliquus superioris*; PR5: pleural rib of fifth vertebra. Scale bar = 1 mm.

Ribs 15(2) or 16(3), last 1(1), 2(2), or 2(3) pairs attached to the haemal arches instead of parapophyses of vertebral centrum. Medial process of first pair of ribs present. Supraneurals 5(2) or 6(3). Epural bones 2(2) or 3(3). Uroneurals 1(5). Total vertebrae 35(4) or 36(1), of which 20 are precaudal and 15 or 16 caudal. Transitional vertebrae 2(2) or 3(2), last one or two with haemal canal.

Coloration in life.—(Figs. 1, 2) Body light brown to olive, with dark-brown vertical bands; ventral region pale to whitish. Dorsal surface light olive. Vertical bands, 7–13 in number, extending from dorsal region, slightly surpassing lateral line. Bands thinner and more numerous in smaller specimens, fusing into broader, fainter bands in larger individuals (Fig. 2). Anterior band positioned behind operculum; posterior band reaching caudal peduncle. Flanks showing gradient from olive dorsally to pastel white ventrally. Vertical bands fading toward mid-ventral region. Interspaces between bands slightly lighter. Faint, diffuse dark brown-gray longitudinal band following lateral line, darker at intersections with vertical bands, fainter in larger specimens.

Head light olive to brown, darker above eye, with subtle mottling around eyes and operculum. Thin, oblique black pre-orbital stripe extending from anteroventral edge of eye to snout tip. Post-orbital stripe absent. Dorsal border of eye dark gray, ventral border pastel white. Iris yellow to orange; pupil black, slightly rounded, with anterior projection toward snout tip. Central opercle golden, with scattered melanophores. Roundish orange spot present posterior to upper opercular border, extending ventrally as light-yellow band toward pectoral-fin insertion. Pattern bordered posteriorly by roundish dark gray spot, followed by lighter gray band extending to posterior border of pectoral-fin base, forming double-dot and double-band orange-gray pattern behind head.

Fins mostly hyaline. Anterior basal portion of dorsal-fin rays, except first, gray. First quarter of dorsal-fin basal portion yellowish to light brown. Lateral dark-brown bands of body extending to dorsal-fin proximal base. Striated appearance more pronounced in smaller specimens. Caudal-fin basal portion marked by thin, light gray, slightly w-shaped band, followed by

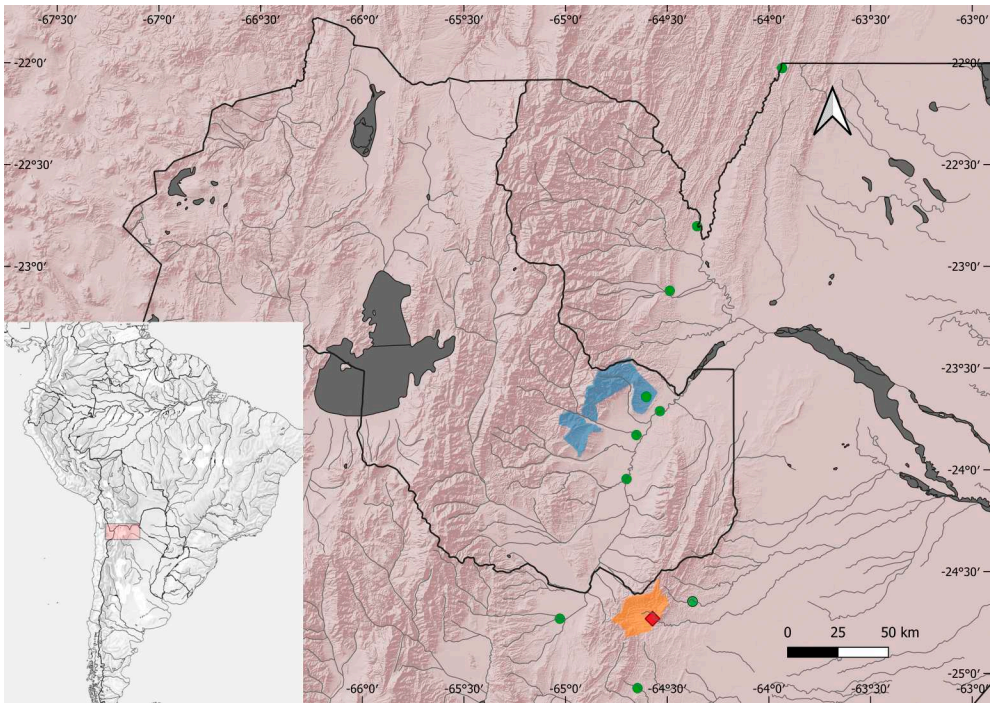

Fig. 7. Distribution map of *Characidium lilloi* in the Andean regions of Bermejo and Juramento basins, showing the type locality (red diamond) and collection sites (green circles). Area in blue represents the National Park Calilegua and in orange the National Park El Rey.

two small gray blotches in central portion; blotches fainter in larger specimens, tending to fuse with basal band. First basal quarter of caudal-fin membrane yellow to brown. Pectoral and pelvic fins mostly hyaline, with minimal pigmentation and pale olive base; rays faintly outlined. Anal fin hyaline, with light olive tint at base, especially around anterior rays.

Coloration of preserved specimens.—Body overall pale brown to grayish, with original vibrant live coloration significantly faded. Banding pattern faint, with reduced contrast compared to live appearance. Ventral surface lighter, nearly white, contrasting with darker dorsal and lateral surfaces. In lateral view, body uniformly pale brown, with faint remnants of vertical bands most visible anteriorly, fading toward caudal peduncle. Scales with slightly darker outlines, imparting a subtle reticulated pattern across flanks.

Dorsal, pectoral, pelvic, and anal fins mostly translucent, with light brown hue; rays slightly darker than membranes. Dorsal surface uniformly light brown to gray, with banding traces weakly visible. Dorsal fin translucent, base with faint brownish pigmentation; rays darker, giving a weakly striated appearance. Head slightly darker than body, with eyes cloudy due to preservation.

Ventral surface lightest, nearly white to pale cream, with minimal pigmentation; belly uniformly light, without visible banding or pattern. Pectoral and pelvic fins nearly hyaline, with minimal pigmentation. Anal fin with faint brown tint. Head light brown to grayish, with minimal contrast to body; operculum slightly darker, showing faint mottling and minimal pattern definition. Eyes clouded and opaque.

Dorsal fin light brown, translucent; rays faintly darker than membranes, creating a subtle striped effect. Caudal fin translucent, continuing body coloration faintly, with minimal patterning. Pectoral and pelvic fins hyaline, with rays slightly pigmented, contributing to a faintly striated appearance. Anal fin with light pigmentation near base; membranes translucent, with slightly darker rays.

Sexual dimorphism.—No distinctive external morphological sexual characters observed between females and males.

Distribution.—*Characidium lilloi* has been recorded from multiple locations in the Andean sections of the Bermejo and Juramento basin in the provinces of Salta and Jujuy, northwestern Argentina (Fig. 7).

Ecological notes.—The species inhabits mountain rivers in the northwestern portion of the La Plata basin, spanning the Andean and sub-Andean mountain ranges. These regions are characterized by the presence of the Yungas jungle and the semiarid Chacoan Forest (Fig. 8). The area experiences distinct rainy and dry seasons, with most rainfall occurring during the summer months, which can reach more than 1,500 mm.

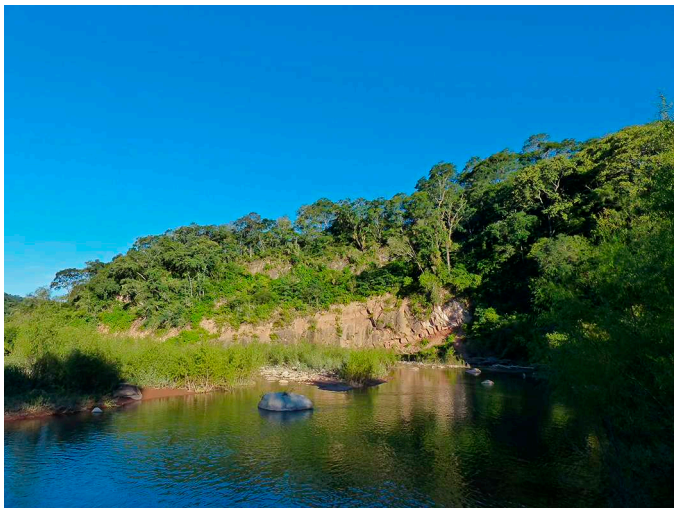

Fig. 8. Popayán River, at the type locality, May 2013 at 24°43′53.8″S, 64°34′21.6″W, Argentina, Salta Province, Anta, Río Popayán at El Rey National Park.

Table 2. Interspecific and intraspecific genetic distances of "*Characidium fasciatum*" clade species and *C. borellii*, under K2 substitution model. Values are represented as percentages.

	1	2	3	4	5	6	7	8	9	Intraspecific distance
1. *C. lilloi*										0.0
2. *C. gomesi*	7.8									0.2
3. *C. fasciatum*	8.0	3.2								0.0
4. *C. dule*	11.0	12.8	13.0							0.1
5. *C. boavistae*	11.3	12.4	12.9	10.5						–
6. *C. marshi*	12.1	14.1	14.2	1.8	10.6					0.1
7. *C. tatama*	12.9	12.5	12.7	8.9	12.3	10.4				0.0
8. *C. bolivianum*	13.5	15.1	14.7	13.9	14.0	14.1	15.1			–
9. *C.* cf. *purpuratum*	14.8	15.6	14.3	15.8	17.9	15.4	17.3	8.7		–
10. *C. borellii*	18.3	19.1	19.0	15.5	18.2	16.6	17.5	17.3	21.0	0.6

Elevations range from approximately 700 to 2,000 meters. During summer, temperatures can reach up to 35°C, while winter minimums average around 10°C (Servicio Meteorológico Nacional; https://www.smn.gob.ar).

Characidium lilloi is typically found in clear-water streams and rivers, although these water bodies can become turbid during summer floods. The species is often observed forming schools near the riverbed in areas with high water flow velocity. In these habitats, it coexists with *Parodon carrikeri* and *Characidium borellii*. The species feeds on the riverbed, adopting a rheotactic position that enables it to maintain stability in fast-flowing waters while feeding, contacting the bottom with its ventral surface and pectoral and pelvic fins (underwater observations made *in situ* and with underwater camera video recordings).

Conservation status.—*Characidium lilloi* faces some environmental pressures, including agrochemical runoff, significant land-cover change due to deforestation in the province of Salta, and industrial discharges into water bodies. However, no major threats have been identified that would pose a significant risk to the species within its known range. The species maintains a broad distribution (Extent of Occurrence ≈ 13,764 km^2) and is particularly abundant in protected areas, such as El Rey National Park and Calilegua National Park, where its habitats remain well preserved.

Given its wide distribution, stable populations, and occurrence in conservation areas, *Characidium lilloi* does not currently meet the criteria for any threatened category. Therefore, based on IUCN guidelines and criteria (IUCN, 2012), the species qualifies for the Least Concern (LC) status.

Etymology.—This species is named in honor of the Argentine naturalist Miguel Lillo (1862–1931), a pioneer who recognized the importance of public investment in science and education. In his commitment to advancing these fields, Lillo donated his personal assets before his death, ensuring the continuity of his legacy through several key institutions. These include the Facultad de Ciencias Naturales e Instituto Miguel Lillo, the Fundación Miguel Lillo, and the Unidad Ejecutora Lillo–CONICET, all of which have played significant roles in the development of science and education in Argentina. The specific name *lilloi*, thus, not only pays tribute to Lillo's contributions but also honors the dedication of public workers in Argentina who promote and contribute to the progress of science, education, and technology.

Molecular Analysis

The final *COI* and *CYTB* alignments were 654 and 747 bp long, respectively.

Pairwise distance.—Inter- and intraspecific distance estimates based on *COI* sequences within the *Characidium fasciatum* clade are provided in Table 2. The species with the closest sequence similarity to *Characidium lilloi* are *C. gomesi* (7.8%) and *C. fasciatum* (8.0%). The most divergent sequences within the clade belong to *C. bolivianum* (13.5%) and *C. purpuratum* (14.8%). In contrast, *C. borellii* (sympatric species of *C. lilloi*) has 18.3% genetic divergence from the new species. The three analyzed sequences of *C. lilloi*—from the Bermejo River, Rey National Park, and the Juramento River basin (CIT-FML 0045, CIT-FML 432, and CIT-FML 707, respectively)—show no intraspecific variation (Table 3).

Phylogeny.—Parsimony analysis (*COI* marker): five most parsimonious treew were obtained for all explored values of K (3, 5, 7, 9, 10, 14, 19, and 27). Under both implied and equal weighting, we recovered *C. lilloi* in a group (*Characidium fasciatum* clade) that also includes *C. boavistae*, *C. bolivianum*, *C. fasciatum*, *C. gomesi*, and *C.* cf. *purpuratum* (consensus tree, K = 10, fit = 89.08158, length = 2,099; Fig. 9A). Regarding the relationships of the new species described herein, both the clade comprising *C. fasciatum*, *C. gomesi*, and *C. lilloi*, and the

Table 3. Specimens of *Characidium lilloi* analyzed in this study, including museum and tissue vouchers, collection localities, and GenBank accession numbers for *COI* and *CYTB* sequences.

Species	Museum voucher	Tissue voucher	Locality	GenBank accession number (*COI*)	GenBank accession number (*CYTB*)
C. lilloi	CI-FML 8196	CIT-FML 432	El Rey National Park	PV799983	
C. lilloi	CI-FML 8199	CIT-FML 707	Juramento River basin	PV799984	
C. lilloi	CI-FML 8123	CIT-FML 045	San Francisco River	PV799982	PV796777

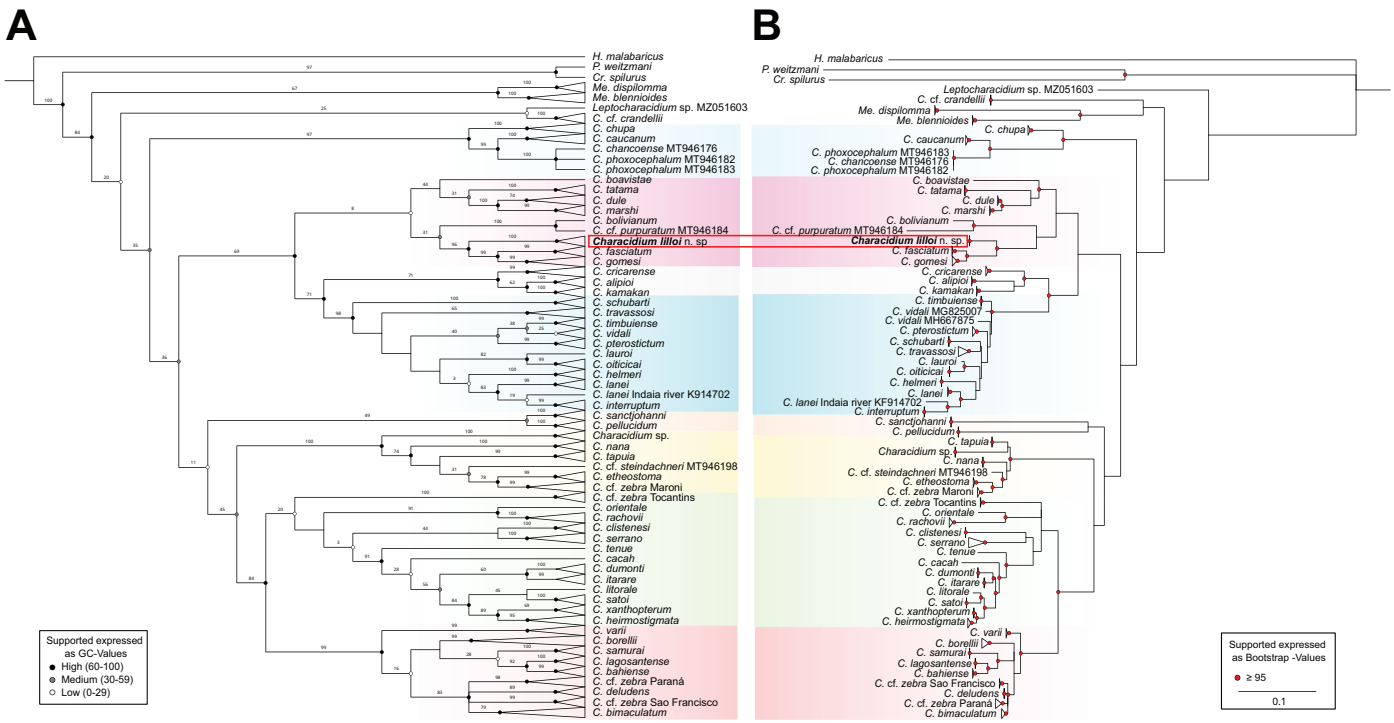

Fig. 9. *COI* phylogenetic trees. (A) Parsimony consensus tree under extended implied weighting (K = 10, length = 2,099, fit = 89.08158), GC supporting values generated from 10,000 replicates. (B) Maximum likelihood tree with TIM2 + F + I + G4 model (Log-likelihood = −9,207.3446; BIC = 20,677.2936), ultrafast bootstrap (UFboot) support values generated from 10,000 bootstrap alignments. See Data Accessibility for tree files.

more restricted clade containing only *C. fasciatum* and *C. gomesi* are highly supported (GC = 96 and GC = 99). *Characidium lilloi* was recovered as a monophyletic clade with high support (GC = 100; Fig. 9A).

Maximum likelihood analysis (*COI* marker): a single tree was obtained under TIM2 + F + I + G4 model (Log-likelihood = −9,207.3446), which was identified as the best-fit model based on the BIC value (BIC = 20,677.2936). It shows a topology similar to that obtained by parsimony for K = 9 to 27 (Fig. 9B). *Characidium lilloi* was also recovered as a monophyletic clade with high statistical support (≥ 95 bootstrap value), and its sister clade was composed of *C. fasciatum* and *C. gomesi* (Fig. 9B).

Combined analysis under parsimony (*COI* + *CYTB* markers): a single most parsimonious tree was obtained under K = 10 (fit = 118.47204, tree length = 2,823). The tree topology was similar than the obtained in previous analyses (parsimony, K = 9 to 27, and ML using only the *COI* marker). All the clades mentioned by Serra et al. (2025) were recovered, with varying degrees of support.

Combined maximum likelihood analysis (*COI* + *CYTB* markers): a single tree was obtained under a partition scheme (Log-likelihood = −13,750.9700; BIC = 28,747.8517). The *Characidium fasciatum* clade was recovered in ML model and exhibit the same topology as the combined analysis under the parsimony and Bayesian models (Fig. 10).

All the clades mentioned by Serra et al. (2025) were recovered in all analyses (also in Bayesian model for only *COI* and *COI* + *CYTB*; Supplemental Text S2; see Data Accessibility), with varying degrees of support.

DISCUSSION

Characidium lilloi is a new species endemic to the upper Bermejo and Juramento basins. *Characidium lilloi* shares the diagnostic characters of clades C1 (cranial fontanel reduced [ch 8: 1], postcleithrum 1 absent [ch 23: 1], unscaled isthmus [ch 43: 1]) and C2 (large pterosphenoid foramen for the ophthalmic nerve [ch 3: 1] and a second vertebral centrum bearing a pair of ventral processes that extend anteroventrally [ch 16: 1]) proposed by Buckup (1993b). Lujan et al. (2013) described *C. amaila*, a species related to clade C1, and determined that although it shares the absence of scales on the isthmus and chest with the *C. fasciatum* group, other internal traits of *C. amaila*—such as a small, channel-like pterosphenoid foramen, absence of ventral processes on the second vertebral centrum, and an elongated posterior chamber of the swimbladder—represent the plesiomorphic condition, implying that the corresponding characters in the *C. fasciatum* group are derived. According to the literature (Buckup, 1992; Lujan et al., 2013), additional diagnostic characters of the *C. fasciatum* group include a pterosphenoid foramen for the ophthalmic nerve centrally located, a foramen largely flat and lacking a bony crest, and a swimbladder with the posterior chamber smaller than the anterior chamber, all of which *Characidium lilloi* exhibits.

Some species, such as *C. dule*, *C. marshi*, and *C. tatama*, have also been recovered within the *C. fasciatum* group in phylogenetic analyses based on mitochondrial markers (Agudelo-Zamora et al., 2020). *Characidium tatama* and *C. dule* both share the diagnostic characters of clade C1—except for the scaled isthmus in *C. dule*—and also present a character not previously evaluated for this group: a concave longitudinal bar that originates at the humeral spot, descends continuously toward the pectoral fin, and extends posteriorly behind the opercle. This character is also present in *C. lilloi* (see Figs. 1, 2).

Molecular analyses also support the phylogenetic placement of *C. lilloi* in this clade. Nevertheless, *Characidium lilloi*

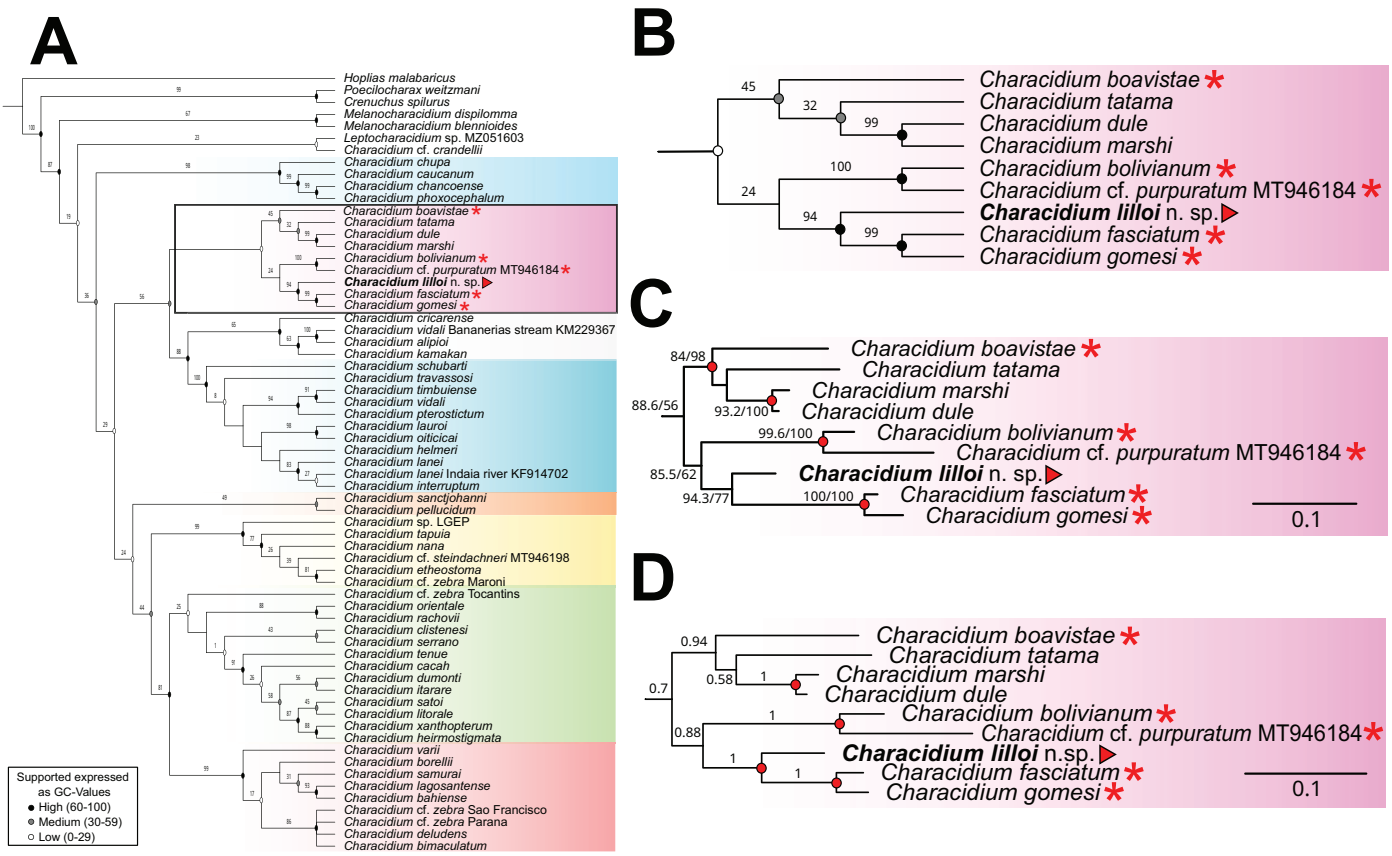

Fig. 10. Trees resulting from the combined analysis of *COI* + *CYTB* markers. (A–B) Under extended implied weighting (K = 10, length = 2,823, fit = 118.47204). GC support values generated from 10,000 replicates. (C) Clade recovered under maximum likelihood analysis (log-likelihood = −13,750.9700). Supported nodes: SH-aLRT ≥ 80% and UFboot ≥ 95%. (D) Clade recovered under Bayesian inference (supported nodes PP > 0.95). Red asterisk: species from the C2 clade of Buckup (1993b). See Data Accessibility for tree files.

exhibits high genetic distances (*COI* marker) compared to other congeners of the C2 clade (*sensu* Buckup, 1993b; *C. gomesi*, 7.8%; *C. fasciatum*, 8.0%; *C. boavistae*, 11.3%; *C. bolivianum*, 13.5%; and *C.* cf. *purpuratum*, 14.8%), underscoring the uniqueness of this taxon as new species. This constitutes the first record of a species belonging to the *Characidium fasciatum* group (clade C2 *sensu* Buckup, 1993b) in Argentina, significantly expanding the known cis-Andean range of this clade and reinforcing the northwestern La Plata basin as an endemicity area.

The complex geological history of the northwestern portion of the La Plata basin—including tectonic uplift, ancient river captures, and vicariant isolation—combined with the region's particular ecological conditions, has played a decisive role in shaping the rich and distinctive ichthyofauna of the area (Terán et al., 2016; Aguilera et al., 2022; Alonso et al., 2024). The upper reaches of the Bermejo and Juramento basins, located along the eastern Andean slopes, are characterized by fast-flowing, clear waters with rocky substrates and sharp altitudinal gradients, with sudden flooding events in the summer rainy season. These environments contrast markedly with the slower, warmer, and sediment-laden lowland rivers of the adjacent Chaco-Pampean plains, where muddy substrates predominate. Such sharp ecological and hydrological transitions act as natural barriers to dispersal, fostering allopatric differentiation and endemism (Calviño and Alonso, 2010; Cancino and Aguilera, 2016; Terán et al., 2016, 2019; Alonso et al., 2024). The result is a biogeographic mosaic in which there are already more than 20 endemic fish species recognized from the upper Bermejo and upper Juramento basins. In addition to *Characidium lilloi*, these include *Andromakhe latens*, *Bryconamericus rubropictus*, *Farlowella azpelicuetae*, *Hoplisoma osvaldoi*, *Jenynsia alternimaculata*, *Jenynsia maculata*, *Jenynsia sulfurica*, *Loricaria holmbergi*, *Microglanis nigrolineatus*, *Nantis indefessus*, *Oligosarcus bolivianus*, *Oligosarcus itau*, *Piabina thomasi*, *Psalidodon chico*, *Psalidodon endy*, *Psalidodon tumbayaensis*, *Urkumayu gladysae*, *Urkumayu micracanthus*, and *Urkumayu petracinii*.

Most of these species have been recently assessed under IUCN criteria and fall within threatened categories due to habitat degradation, narrow ranges, and anthropogenic pressure. Common threats include deforestation, water pollution from sewage and agrochemicals, open garbage dumps, and agricultural expansion. In contrast, *Characidium lilloi* currently faces no major threats, as its populations are located within El Rey and Calilegua National Parks, where environmental protection ensures stable conditions. Accordingly, the species meets the criteria for Least Concern (LC) under the IUCN Red List (IUCN, 2012). However, its range should continue to be monitored, especially in areas outside the boundaries of these reserves.

The occurrence of *Characidium lilloi*, *C. borellii*, *Nantis indefessus*, and *Rineloricaria steinbachi* in both the Bermejo and Juramento basins suggests historic hydrographic connectivity, possibly driven by Pleistocene or Holocene river captures in the Lerma Valley (Monasterio, 2003; Aguilera et al., 2022).

The morphology of *Characidium lilloi*—elongated body, shallow body depth, reduced ventral squamation, decrease swimbladder size, large pectoral and anal fins set ventrally, and a straight ventral surface—reflects adaptations to rheophilic environments. This body plan enhances hydrodynamic efficiency in turbulent waters and promotes benthic station-holding behavior, a pattern well documented in other lotic-adapted taxa (Carlson and Lauder, 2010; Lujan and Conway, 2015; Zanata et al., 2020). Behavioral observations in the field revealed that individuals of *C. lilloi* swim close to the substrate, using their paired fins to attach to the bottom and stabilize against the current while foraging. These adaptations are not exclusive to *C. lilloi*, but are also observed in other members of clade C1, which exhibit several morphological specializations associated with rheophily; among them, the most notable is the absence of scales on the isthmus. The adaptive advantage of reduced ventral squamation remains uncertain, although it has been hypothesized that scales may simply hinder close contact with the substrate (Lujan and Conway, 2015).

As environmental changes continue to affect South American freshwater systems, research efforts should be directed toward discovering undocumented diversity and implementing conservation measures grounded in sound taxonomic knowledge (Terán et al., 2020). Ultimately, the discovery of *Characidium lilloi* contributes to our understanding of the biogeography, evolution, and ecological complexity of the northwestern La Plata River basin. It also highlights the value of integrative taxonomy—combining morphology, osteology, and molecular data—for recognizing lineages and refining systematic frameworks.

MATERIAL EXAMINED

Comparative material listed in Serra et al. (2025) and Méttola et al. (2025); additional material listed below.

Characidium alipioi: All from Brazil, São Paulo, Rio Paraiba do Sul system. MZUSP 109873, 1, 78.6 mm SL; MZUSP 112331, 6, 48.7–70.5 mm SL; MZUSP 79427, 25, 70–86.2 mm SL.

Characidium bimaculatum: MZUSP 68959, 3 (1 CS), 20.2–25.3 mm SL, Brazil, Rio Grande do Norte, Rio Ceara-Mirim.

Characidium boavistae: All from Colombia. IAvH-P-9760, 16, 37.5–49.4 mm SL, Norte de Santander, río Catatumbo, Lago de Maracaibo basin; IAvH-P-9767, 26, 31–46.4 mm SL, Norte de Santander, río Catatumbo, Lago de Maracaibo basin; IAvH-P-11801, 19, 38.1–49.8 mm SL, Norte de Santander, Río Zulia, Lago de Maracaibo basin; IAvH-P-21619, 3, 29.8–38.5 mm SL, Meta, Río Meta, Orinoco basin; IAvH-P-23640, 8, 33.9–44.1 mm SL, Meta, Río Meta, Orinoco basin; IAvH-P-29935, 1, 40.9 mm SL, Putumayo, Río Putumayo, Amazonas basin.

Characidium bolivianum: All from Bolivia, La Paz, Río Beni system, Amazonas basin. CBF 16934, 1 (tissue voucher: T071), 30.5 mm SL, Franz Tamayo, Río Tuichi; GMC.IM.AMA.MAD-1, 1, 32.8 mm SL, Iturralde, Río Madidi; GMC.IM.AMA.PAC-1, 1, 40.5 mm SL, Iturralde, Arroyo Pacú; GMC.IM.HON.ESM-1, 4, 33.1–44.3 mm SL, Franz Tamayo, Arroyo Esmeralda; GMC.IM.HON.HON-2, 3, 34.3–35.7 mm SL, Franz Tamayo, Río Hondo; GMC.IM.HON.HON-4, 1, 45.3 mm SL, Franz Tamayo, Río Hondo; GMC.IM.HON.HON-5, 1, 60. 8 mm SL, Franz Tamayo, Río Hondo; GMC.IM.HON.HON-7, 2, 38.4–38.6 mm SL, Franz Tamayo, Río Hondo; GMC.IM.HON.HON-8, 2, 19–22.2 mm SL, Franz Tamayo, Río Hondo; GMC.IM.HON.LRUT-1, 1, 24.5 mm SL, Franz Tamayo, Laguna Ruta; GMC.IM.-HON.PER-1, 4, 32.3–42.1 mm SL, Franz Tamayo, Arroyo Perla; GMC.IM.SIP.MAC-1, 4, 55.7–66 mm SL, Franz Tamayo, Río Machariapo; GMC.IM.SIP.TUI-CUA, 1, 53.2 mm SL, Franz Tamayo, Río Tuichi; GMC.IM.SIP.UBI-2, 3, 32.3–75.3 mm SL, Franz Tamayo, Río Ubito; GMC.IM.SIP.UBI-1, 1, 57.2 mm SL, Franz Tamayo, Río Ubito; GMC.IM.SIP.UBI-3, 1, 32.6 mm SL, Franz Tamayo, Río Ubito.

Characidium borellii: CI-FML 3865, 103 (3 CS), 42.9–53.6 mm SL, Argentina, Tucumán, Río Salí-Dulce, La Plata basin.

Characidium caucanum: IAvH-P-1520, 1, 43.8 mm SL, Colombia, Quindío, Río La Vieja, Magdalena-Cauca basin.

Characidium crandellii: IAvH-P-20573, 3, 38.7–41.7 mm SL, Colombia, Vaupés, Río Caqueta system, Amazonas basin.

Characidium deludens: All from Brazil, Bahia, Rio Paraguaçu basin. MZUSP 115009, 1, holotype, 48.1 mm SL; MZUSP 115010, 9, paratypes, 27–40.9 mm SL.

Characidium dule: IAvH-P-13334, 42, 28.18–42.12 mm SL, Colombia, Chocó, Río Unguía, Atrato basin.

Characidium fasciatum: All from Brazil. MZUSP 37067, 2, 42.4–48.8 mm SL, São Paulo, Rio Claro, Paraná basin; MZUSP 85981, 13, 21.4–35.6 mm SL, Minas Gerais, Rio Verde Grande, rio São Francisco basin; MZUSP 85995, 32 (1 CS), 22.6.26.3 mm SL, Minas Gerais, Rio Verde Grande, Rio São Francisco basin.

Characidium gomesi: All from Brazil. MZUSP 88349, 6, 31.2–38.7 mm SL, Mato Grosso do Sul, Rio Sucuriú Paraná basin; MZUSP 110032, 3, 31.1 mm SL, Minas Gerais, rio Araguari system, Paraná basin; MZUSP 110447, 6, 32.9–59.3 mm SL, Minas Gerais, rio Paranaíba system, Paraná basin.

Characidium lagosantense: MZUSP 73708, 2, 19.3–22.9 mm SL, Brazil, Minas Gerais, Río Cipó, Rio São Francisco basin.

Characidium lanei: All from Brazil, São Paulo. MZUSP 114844, 11, 28.9–46.3 mm SL, Itanhaém; MZUSP 120519, 1, 41.8 mm SL, Cachoeira do Pitu, Itapitangui.

Characidium lauroi: All from Brazil, São Paulo, Rio Paraíba do Sul basin. MZUSP 110359, 5, 30.8–45 mm SL, Bananal, Rio das Cobras; MZUSP 124033, 12, 37.4–49.1 mm SL, Ribeirão Grande.

Characidium litorale: All from Brazil, Rio de Janeiro, Rio São João system. MZUSP 129926, 2, 18.8–25 mm SL, Rio Aldeia Velha; MZUSP 129946, 1, 34.35 mm SL, Casimiro De Abreu, Rio Aldeia Velha.

Characidium nana: MZUSP 125919, 10, 15.8–20.7 mm SL, Brazil, Pará, Altamira, Rio Xingú, Amazonas basin.

Characidium nupelia: All from Brazil, Mato Grosso, Paraguay system, La Plata basin. MZUSP 87743, 1, holotype, 28.9 mm SL, Rio Manso; MZUSP 87742, 20, paratypes, 21.8–28.9 mm SL, Rio Manso.

Characidium oiticicai: All from Brazil, São Paulo. MZUSP 87716, 3, 34–44.8 mm SL, Salesópolis, Ribeirão do Campo,

Rio Tieté, Paraná basin; MZUSP 110245, 14, 23.2–55.7 mm SL, Salesópolis, Rio Paraitinga, Rio Paraiba do Sul basin.

Characidium onca: All from Brazil, Distrito Federal, Brasilia. MZUSP 125807, 1, holotype, 39.7 mm SL, Lago Paranoá, bacia do rio São Bartolomeu; MZUSP 125803, 6 (2 CS), paratypes, 26.8–30.5 mm SL, Lago Paranoá, bacia do rio São Bartolomeu.

Characidium phoxocephalum: All from Colombia, Caldas, Río La Miel, Magdalena basin. IAvH-P-8432, 1, 53.9 mm SL; IAvH-P-8434, 1, 89.7 mm SL.

Characidium pterostictum: CI-FML 8189, 11, 26.6–54.9 mm SL, Argentina, Corrientes, Santo Tome, Arroyo Ciriaco, Uruguay system, La Plata basin.

Characidium purpuratum: All from Ecuador, Pastaza, Río Bobonaza Marañon system, Amazon basin. MEPN-I 1077, 2, 43.3–46.1 mm SL; MEPN-I 1117, 1, 37.87 mm SL.

Characidium rachovii: All from Argentina, Tucumán, Salí-Dulce system, La Plata basin. CI-FML 3866, 1, 30.9 mm SL, Río Mandolo; CI-FML 5372, 1, 28.7 mm SL, Arroyo Los Perez.

Characidium schubarti: MZUSP 71023, 3, 34.2–42.7 mm SL, Brazil, São Paulo, Riacho Barra Grande, Rio Ribeira de Iguape system.

Characidium stigmosum: MZUSP 40804, 1, paratypes, 27.9–35.5 mm SL, Brazil, Goiás, Rio Maranhão system, Tocantins basin.

Characidium travassosi: All from Brazil, Paraná, Rio Iguaçú, Parana basin. MZUSP 85940, 1, holotype, 33.7 mm SL; MZUSP 85938, 6 (1 CS), paratypes, 32.6–33.3 mm SL.

Characidium tenue: All from Argentina, Corrientes, Uruguay system, La Plata basin. CI-FML 8187, 1, 29.9 mm SL, Arroyo Guaviravi; CI-FML 8188, 1, 29.1 mm SL, Arroyo Morredor.

Characidium xanthopterum: MZUSP 41454, 20, 21.6–31.3 mm SL, Brazil, Mato Grosso, Rio Itiquira, Paraguay system, La Plata basin.

Characidium zebra: All from Brazil, Roraima, Rio Branco drainage, Amazonas basin. MZUSP 117743, 5, 30.8–39.3 mm SL, Rio Arraias; MZUSP 117946, 1, 33.6 mm SL, Rio Cauame.

Characidium aff. *zebra*: CI-FML 7680, 7, 26.8–37.2 mm SL, Argentina, Corrientes, Arroyo Pehuajo, Paraná, system, La Plata basin.

Melanocharacidium dispilomma: All from Colombia, Orinoco basin. IAvH-P-12885, 27, 21.22–31.65 mm SL, Vichada, Caño Juriepe, Río Meta system; IAvH-P-26305, 6, 27.5–33.8 mm SL, Meta, Río Vichada drainage.

DATA ACCESSIBILITY

Supplemental material is available at https://www.ichthyologyandherpetology.org/i2025064. Unless an alternative copyright or statement noting that a figure is reprinted from a previous source is noted in a figure caption, the published images and illustrations in this article are licensed by the American Society of Ichthyologists and Herpetologists for use if the use includes a citation to the original source (American Society of Ichthyologists and Herpetologists, the DOI of the *Ichthyology & Herpetology* article, and any individual image credits listed in the figure caption) in accordance with the Creative Commons Attribution CC BY License. ZooBank publication urn:lsid:zoobank.org:pub:5FB9AFF4-B64C-42F0-BDE0-46C3B6B57FF0.

AI STATEMENT

The authors declare that ChatGPT (OpenAI) and Gemini 2.5 Pro were used to assist with grammar correction, language polishing, and reference formatting. It was not used to generate or analyze data in this manuscript. These tools were used under full human supervision and critical review. The authors remain solely responsible for the scientific interpretation, methodological decisions, and the intellectual content of the work.

ACKNOWLEDGMENTS

We are grateful to the Secretaría de Ambiente y Desarrollo Sustentable of Salta Province, particularly Yanina Bonduri and Sebastián Musalem (Res. 101/2023), and to the National Parks Administration (DRNOA 149/2018), for granting the necessary collecting permits. We also thank the Ministerio de Ambiente y Cambio Climático of Jujuy for the permit (Permit 1103-306-M/2016). All procedures used in this study complied with current regulations and adhered to the Guide for the Care and Use of Laboratory Animals (CONICET, 2011), and were approved under the corresponding permits. We thank Fundación ProYungas and the Ledesma Group—especially Arturo Blanco—for logistical support and assistance. We acknowledge IBIGEO and Fundación Miguel Lillo for their continued institutional support. We thank Miguel Casalinuovo (in memoriam) for providing some of the specimens and for his help during the sampling trips. We thank the members of the Killifish Foundation, as well as Fernando Lobo, Baltazar Bugeau, Roberto Sánchez, Julio Cruz, and Virginia Martínez for their ongoing assistance and encouragement. We are indebted to Ana Sofía Méttola for her help with image editing. We also thank Jon Fong for providing photographs of type specimens of *Characidium zebra* and *C. bolivianum*. TNT software was provided free of charge by the Willi Hennig Society.

This study was partially supported by the National Scientific and Technical Research Council of Argentina (CONICET), through project PIBAA 2872021010 0128CO, and by a grant from Fundación Williams ("Fondos complementarios para la investigación con impacto en el territorio argentino: Peces de la cuenca del Río Bermejo: biodiversidad, distribución espaciotemporal, efectos de las actividades antrópicas y conservación") awarded to F. Alonso.

Additional funding was provided by the Agencia Nacional de Promoción de la Investigación, el Desarrollo Tecnológico y la Innovación (ANPCyT) through grants to J. M. Mirande (PICT-2020-02141) and G. Aguilera (PICT-2019-01004), as well as by CONICET through a grant to J. M. Mirande (PIP-2020-0101214). The manuscript benefited greatly from the constructive comments of three anonymous reviewers.

Author contributions—Conceptualization: GET, VEM, GA, JMM; Data Curation: GET, VEM, GM; Formal Analysis: VEM, GET, MMM; Funding Acquisition: GA, FA, GET, JMM; Investigation: GET, VEM, FA, MMM, AML, GM, GA, JMM; Methodology: GET, VEM, FA, MMM, AML, GM, GA, JMM; Visualization: AML, VEM, GET; Writing—Original Draft: GET, VEM, FA; Writing—Review and Editing: GA, VEM, GET, FA, MMM, AML, JMM.

LITERATURE CITED

Agudelo-Zamora, H. D., J. Tavera, Y. D. Murillo, and A. Ortega-Lara. 2020. The unknown diversity of the genus *Characidium* (Characiformes: Crenuchidae) in the Chocó biogeographic region, Colombian Andes: two new species supported by morphological and molecular data. Journal of Fish Biology 97:1662–1675.

Aguilera, G., G. E. Terán, A. Méndez-López, M. M. Montes, and T. P. Carvalho. 2025. A new species of the banjo catfish genus *Ernstichthys* (Siluriformes: Aspredinidae) from the Bermejo River Drainage, La Plata Basin, Argentina. Ichthyology & Herpetology 113:527–539.

Aguilera, G., G. E. Terán, J. M. Mirande, F. Alonso, G. Miranda Chumacero, Y. Cardoso, S. Bogan, and D. R. Faustino-Fuster. 2022. An integrative approach method reveals the presence of a previously unreported species of *Imparfinis* Eigenmann and Norris 1900 (Siluriformes: Heptapteridae) in Argentina. Journal of Fish Biology 101:1248–1261.

Aguilera, G., G. E. Terán, J. M. Mirande, F. Alonso, S. Rometsch, A. Meyer, and J. Torres-Dowdall. 2019. Molecular and morphological convergence to sulfide-tolerant fishes in a new species of *Jenynsia* (Cyprinodontiformes: Anablepidae), the first extremophile member of the family. PLoS ONE 14:e0218810.

Alonso, F., G. E. Terán, G. Aguilera, M. M. Montes, W. S. Serra Alanís, P. Calviño, H. S. Vera-Alcaraz, Y. Cardoso, S. Koerber, and J. M. Mirande. 2024. Integrative phylogeny of Corydoradinae (Siluriformes: Callichthyidae) with an emphasis on northwestern La Plata species, including descriptions of a new genus and species. Zoologischer Anzeiger 314:10–23.

Buckup, P. A. 1992. Redescription of *Characidium fasciatum*, type species of the Characidiinae (Teleostei, Characiformes). Copeia 1992:1066–1073.

Buckup, P. A. 1993a. Review of the genus *Characidium* Reinhardt (Teleostei: Characidiinae) with description of two new species. Ichthyological Exploration of Freshwaters 4:97–120.

Buckup, P. A. 1993b. Phylogenetic interrelationships and reductive evolution in the neotropical characidiin fishes (Characiformes, Ostariophysi). Cladistics 9:305–341.

Calviño, P. A., and F. Alonso. 2010. Two new species of genus *Corydoras* (Ostariophysi: Siluriformes: Callichthyidae) from northwest Argentina, and redescription of *C. micracanthus* Regan, 1912. Revista del Museo Argentino de Ciencias Naturales 11:199–214.

Cancino, F., and G. Aguilera. 2016. Ictiofauna, p. 40–46. *In*: Biodiversidad y Fronteras: Cuenca del Río Bermejo (Salta, Argentina). Serie Conservación de la Naturaleza. No. 21. C. Antelo, E. Bulacio, F. Cancino, N. Marigliano, M. Peralta, G. Ramallo, and F. Romero (eds.). Fundación Miguel Lillo, San Miguel de Tucumán.

Carlson, R. L., and G. V. Lauder. 2010. Living on the bottom: kinematics of benthic station-holding in darter fishes (Percidae: Etheostomatinae). Journal of Morphology 271:25–35.

Chernomor, O., A. Von Haeseler, and B. Q. Minh. 2016. Terrace aware data structure for phylogenomic inference from supermatrices. Systematic Biology 65:997–1008.

Díaz, J., G. V. Villanova, F. Brancolini, F. Del Pazo, V. M. Posner, A. Grimberg, and S. E. Arranz. 2016. First DNA barcode reference library for the identification of South American freshwater fish from the lower Paraná River. PLoS ONE 11:e0157419.

Edgar, R. C. 2004. MUSCLE: multiple sequence alignment with high accuracy and high throughput. Nucleic Acids Research 32:1792–1797.

Fink, S. V., and W. L. Fink. 1981. Interrelationships of the ostariophysan fishes (Teleostei). Zoological Journal of the Linnean Society 72:297–353.

Fink, S. V., and W. L. Fink. 1996. Interrelationships of the ostariophysan fishes (Teleostei), p. 209–249. *In*: Interrelationships of Fishes. M. L. J. Stiassny, L. R. Parenti, and G. D. Johnson (eds.). Academic Press, San Diego, California.

Flausino Junior, N., F. C. T. Lima, F. A. Machado, and M. R. S. Melo. 2020. A new species of *Characidium* Reinhardt (Characiformes: Crenuchidae) with a unique mid-water behavior from the upper rio Madeira basin, Brazil. Zootaxa 4816:350–360.

Goloboff, P. A. 1993. Estimating character weights during tree search. Cladistics 9:83–91.

Goloboff, P. A. 2014. Extended implied weighting. Cladistics 30:260–272.

Goloboff, P. A, J. S. Farris, M. Källersjö, B. Oxelman, M. J. Ramiréz, and C. A. Szumik. 2003. Improvements to resampling measures of group support. Cladistics 19:324–332.

Hoang, D. T., O. Chernomor, A. Von Haeseler, B. Q. Minh, and L. S. Vinh. 2018. UFBoot2: improving the ultrafast bootstrap approximation. Molecular Biology and Evolution 35:518–522.

IUCN. 2012. IUCN Red List Categories and Criteria: Version 3.1. Second edition. International Union for Conservation of Nature.

Kalyaanamoorthy, S., B. Q. Minh, T. K. Wong, A. Von Haeseler, and L. S. Jermiin. 2017. ModelFinder: fast model selection for accurate phylogenetic estimates. Nature Methods 14:587–589.

Kumar, S., G. Stecher, M. Li, C. Knyaz, and K. Tamura. 2018. MEGA X: molecular evolutionary genetics analysis across computing platforms. Molecular Biology and Evolution 35:1547–1549.

Loureiro, M., R. de Sá, S. W. Serra, F. Alonso, L. E. Krause Lanés, M. Vieira Volcan, P. Calviño, D. Nielsen, A. Duarte, and G. Garcia. 2018. Review of the family Rivulidae (Cyprinodontiformes, Aplocheiloidei) and a molecular and morphological phylogeny of the annual fish genus *Austrolebias* Costa 1998. Neotropical Ichthyology 16:e180007.

Lujan, N. K., H. Agudelo-Zamora, D. C. Taphorn, P. N. Booth, and H. López-Fernández. 2013. Description of a new, narrowly endemic South American darter (Characiformes: Crenuchidae) from central Guiana shield highlands of Guyana. Copeia 2013:454–463.

Lujan, N. K., and K. Conway. 2015. Life in the fast lane: a review of rheophily in freshwater fishes, p. 107–136 and 297–307. *In*: Extremophile Fishes: Ecology, Evolution, and Physiology of Teleosts in Extreme Environments. R. Riesch, M. Tobler, and M. Plath (eds.). Springer, Cham.

Melo, M. R., and O. T. Oyakawa. 2015. A new species of *Characidium* Reinhardt (Characiformes, Crenuchidae) with a distinctively dimorphic male. Ichthyology & Herpetology 103:281–289.

Méttola, V. E., G. E. Terán, G. Aguilera, M. M. Montes, M. Ibañez Shimabukuro, F. Alonso, J. M. Mirande. 2025. Integrative study of *Characidium borellii* (Characiformes:

Crenuchidae): phylogenetic relationships and geographic distribution. Neotropical Ichthyology 23:e250022.

Mirande, J. M., G. Aguilera, and M. M. Azpelicueta. 2004. A new genus and species of small characid (Ostariophysi, Characidae) from the upper río Bermejo basin, northwestern Argentina. Revue Suisse de Zoologie 111:715–728.

Mirande, J. M., G. Aguilera, and M. M. Azpelicueta. 2006. *Astyanax endy* (Characiformes: Characidae), a new fish species from the upper Río Bermejo basin, northwestern Argentina. Zootaxa 1286:57–68.

Mirande, J. M., G. Aguilera, and M. M. Azpelicueta. 2011. A threatened new species of *Oligosarcus* and its phylogenetic relationships, with comments on *Astyanacinus* (Teleostei: Characidae). Zootaxa 2994:1–20.

Monasterio, L. 2003. Caracterización morfosedimentológica del río Bermejo y sus afluentes en la provincia de Salta. Revista de Geografía Norte Grande 30:69–86.

Nelson, G. J. 1969. Gill arches and the phylogeny of fishes with notes on the classification of the vertebrates. Bulletin of the American Museum of Natural History 141:475–522.

Nelson, G. J. 1973. Relationships of the Clupeomorpha, with remarks on the structure of the lower jaw in fishes. Zoological Journal of the Linnean Society 53(supplement): 333–349.

Oliveira-Silva, L., H. Batalha-Filho, P. Camelier, and A. M. Zanata. 2024. Underestimated diversity in *Characidium* (Characiformes: Crenuchidae) from Neotropical rivers revealed by an integrative approach. Systematics and Biodiversity 22:2346510.

Palumbi, S., A. Martin, S. Romano, W. O. McMillan, L. Stice, and G. Grabowski. 1991. The simple fool's guide to PCR. Department of Zoology and Kewalo Marine Laboratory, University of Hawaii, Honolulu.

Roberts, T. R. 1969. Osteology and relationships of characoid fishes, particularly the genera *Hepsetus*, *Salminus*, *Hoplias*, *Ctenolucius* and *Acestrorhynchus*. Proceedings of the California Academy of Sciences 36:391–500.

Sabaj, M. H. 2020. Codes for natural history collections in ichthyology and herpetology. Copeia 108:593–669.

Serra, W., F. Scarabino, V. E. Méttola, M. M. Montes, G. E. Terán, M. Moncada, and M. García. 2025. *Characidium serrano* Buckup & Reis, 1997 (Characiformes, Crenuchidae): insights into phylogenetic relationships, and comments on distribution. Acta Zoológica Lilloana 69:1–28.

Souza-Shibatta, L., J. F. R. Tonini, V. P. Abrahao, L. R. Jarduli, C. Oliveira, L. R. Malabarba, S. H. Sofia, and O. A. Shibatta. 2018. Reappraisal of the systematics of *Microglanis cottoides* (Siluriformes, Pseudopimelodidae), a catfish from southern Brazil. PLoS ONE 13:e0199963.

Stabile, B. H. M., R. B. Reis, A. Frota, W. D. Graça, and A. D. Oliveira. 2024. Morphology and molecular evidence of a new species of *Characidium* (Characiformes: Crenuchidae) from the edges of a protected area at Rio Itararé, upper Rio Paraná, southern Brazil. Journal of Fish Biology 105:1850–1861.

Stabile, B. H. M., R. B. Reis, A. V. Oliveira, and W. J. Graça. 2025. A new species of *Characidium* (Characiformes: Crenuchidae) from the Iguaçu National Park, Rio Iguaçu basin, Paraná, Brazil. Journal of Fish Biology 107:454–465.

Taylor, W., and G. C. Van Dyke. 1985. Revised procedures for staining and clearing small fishes and other vertebrates for bone and cartilage study. Cybium 9:107–119.

Terán, G. E., G. A. Ballen, F. Alonso, G. Aguilera, and J. M. Mirande. 2019. A new species of *Farlowella* (Siluriformes: Loricariidae) from the upper Bermejo River, La Plata River basin, northwestern Argentina. Neotropical Ichthyology 17:e180114.

Terán, G. E., M. F. Benítez, and J. M. Mirande. 2020. Opening the Trojan horse: phylogeny of *Astyanax*, two new genera, and resurrection of *Psalidodon* (Teleostei: Characidae). Zoological Journal of the Linnean Society 109:1217–1234.

Terán, G. E., L. R. Jarduli, F. Alonso, J. M. Mirande, and O. A. Shibatta. 2016. *Microglanis nigrolineatus*, a new species from northwestern Argentina (Ostariophysi: Pseudopimelodidae). Ichthyological Exploration of Freshwaters 27:193–202.

Travassos, H. 1952. Contribuição ao estudo da subordem Characoidei Berg, 1940. IX–Sôbre o subgênero Jobertina Pellegrin, 1909, com uma nova subfamília (Actinopterygii, Cypriniformes). Boletim do Museu Nacional (série Zoologia) 109:1–45, pls. 1–9.

Trifinopoulos, J., L. T. Nguyen, A. Haeseler, and B. Q. Minh. 2016. W-IQ-TREE: a fast online phylogenetic tool for maximum likelihood analysis. Nucleic Acids Research 44:232–235.

Ward, R. D., T. S. Zemlak, B. H. Innes, P. R. Last, and P. D. Hebert. 2005. DNA barcoding Australia's fish species. Philosophical Transactions of the Royal Society B 360: 1847–1857.

Weitzman, S. H. 1962. The osteology of *Brycon meeki*, a generalized characid fish, with an osteological definition of the family. Stanford Ichthyological Bulletin 8:3–77.

Zanata, A. M., W. M. Ohara, O. T. Oyakawa, and F. Dagosta. 2020. A new rheophilic South American darter (Crenuchidae: *Characidium*) from the rio Juruena basin, Brazil, with comments on morphological adaptations to life in fast-flowing waters. Journal of Fish Biology 97:1387–1402.

Zanata, A. M., C. Oliveira, and L. Oliveira-Silva. 2024. Integrative taxonomy reveals a new species of *Characidium* (Characiformes: Crenuchidae) shared by tributaries of upper Tapajós and Xingu River basins, Brazil. Journal of Fish Biology 105:1929–1938.